Influence of polymer architecture and polymer-wall interaction on the adsorption of polymers into a slit-pore

Zhong Chen and Fernando A. Escobedo*
School of Chemical Engineering, Cornell University, Ithaca, New York, 14850-5201, USA
(Received 25 August 2003; published 17 February 2004)

The effects of molecular topology and polymer-surface interaction on the properties of isolated polymer chains trapped in a slit were investigated using off-lattice Monte Carlo simulations. Various methods were implemented to allow efficient simulation of molecular structure, confinement force, and free energy for a chain interacting with such ''sticky'' surfaces. The simulations were performed in the canonical ensemble, and the free energy was sampled via virtual slit-separation moves. Six different chain architectures were studied: linear, star-branched, dendritic, cyclic, two-node (i.e., containing two tetrafunctional intramolecular crosslinks), and six-node molecules. The first three topologies entail increasing degrees of branching, and the last three topologies entail increasing degrees of intramolecular bonding. The confinement force, monomer density profile, and conformational properties for all these systems were compared (for identical molecular weight N) and analyzed as a function of adsorption strength. The compensation point where the wall attraction counterbalances the polymer-slit exclusion effects was the focus of our study. It was found that the attractive energy at the compensation point, ε_c, is a weak increasing function of the chain length for excluded-volume chains. The value of ε_c differs significantly for different topologies, and smaller values are associated with better-adsorbing molecules. Due to their globular shape and numerous chain ends, branched molecules (e.g., stars and dendrimers) experience a relatively small entropic penalty for adsorption at low adsorption force and moderate confinement. However, as the adsorption force increases, the more flexible linear chains reach the compensation point at a weaker attractive energy because of the ease with which monomers can be packed near the walls. In moderate to weak confinement, molecules with intramolecular cross-links, such as cyclic, two-node, and six-node molecules, always adsorb better than the other chains (with the same N). Especially at strong adsorption, two-node and six node molecules are highly localized in the region near the walls. Under strong confinement conditions, chain rigidity becomes the dominating factor and the more flexible linear chain adsorbs the best at all adsorption strengths. These results provide useful insights for controlling confinement and depletion forces of polymers with different molecular architectures in the presence of attractive polymer-surface interactions.

DOI: 10.1103/PhysRevE.69.021802 PACS number(s): 36.20.−r

I. INTRODUCTION

The conformational and thermodynamic properties of polymer chains are strongly affected by geometric confinement. This phenomenon is relevant to numerous applications of polymers, as in chromatographic separations, colloidal stabilization, thin-film processing, and the preparation of clay-based nanocomposites.

While rigorous formulations exist for the configurational properties and partitioning of a Gaussian chain in pores [1], a rigorous analytical theory has not been worked out for excluded-volume (EV) chains (a model adequate to describe good solvent conditions), and only approximate theories are available, e.g., mean field theory [2] and scaling theory [3]. Scaling theory has had the most general applicability so far, although it is valid for limiting conditions and can give only semiquantitative predictions. Most of the theoretical and simulation work on confined polymers so far has been concerned with linear chains; studies on polymers with more complicated topology are very limited. It is well known that polymers with complex internal architecture have quite different static and dynamic properties. The question then arises as to how the internal architecture affects the properties of confined polymer chains. Just as in the case of linear polymers, rigorous theoretical solutions are available for an ideal self-crossing cyclic chain confined in slitlike pores [4] and scaling results are available for a cyclic EV chain [5]. These theories predict substantial differences in the partition coefficients of linear and cyclic macromolecules under weak adsorption conditions, opening up the possibility for the development of a method for separating cyclic and linear polymers [6]. An on-lattice simulation study was carried out for the adsorption of polymer chains with different molecular architectures, including linear, star, and cyclic chains, on a solid surface [7]. For weakly adsorbed chains it was shown that ring polymers are always adsorbed ca. 50% more than linear and star-branched ones, while the properties of adsorbed linear and star polymers are very similar. Experimental work in this area has been even more scarce [8].

In a previous paper [9], we investigated the properties of topologically complex polymers, such as rings, stars, dendrimers, and hyperbranched polymers, confined in repulsive slit-pores. It was found that scaling theory for linear chains well describes all the properties of star molecules examined and the scaling of the linear dimensions of dendrimers and hyperbranched polymers. The relative partition coefficient at the dilution limit was estimated from the data of F vs slit separation D. It was shown that for very narrow D branched polymers tend to be depleted in the pore relative to linear

*Corresponding author. Email address: fe13@cornell.edu

chains with the same molecular weight. This is due to the fact that branched chains tend to have a higher average monomer concentration inside the polymer coil and experience a larger entropic penalty than linear chains upon strong confinement. However, at large D, branched chains tend to be concentrated in the pore relative to linear chains, which can be explained by the smaller radius of gyration (R_g) of the branched chain coils.

As an extension to our previous work, the effect of attractive interactions between polymer beads and slit walls is considered in this paper. The introduction of an adsorption force is of significance not only from a practical point of view (e.g., it corresponds to liquid adsorption chromatography), but also from a theoretical standpoint, as it provides a platform to investigate the interplay among confinement entropy, adsorption enthalpy, and molecular topology in a confined environment. This interplay is especially important in the adsorption critical regime where the energy gain due to adsorption compensates the entropy loss due to the confinement. The critical adsorption for the linear Gaussian chain was studied theoretically [10], and the compensation point was predicted to be independent of chain length. However, for nonideal chains, the compensation point was found to be a weak function of chain length via computer simulations [11,12]. Using the matrix generation method, Guttman, Di Marzio, and Douglas [13] examined the critical adsorption conditions for homopolymers, block copolumers, stars, and comblike polymers with no excluded-volume interactions. At the critical adsorption condition, it is expected that chain topology will have a major impact on the partitioning of polymer solutions. By sequentially studying entropic and energetic effects, the effect of molecular topology on the partition coefficient can be understood more clearly and this may lead to applications in the technology of polymer fractionation.

In this work, the adsorption force is described by the Steele potential energy function [14]. By varying the polymer-wall adsorption energy parameter ε, the simulation can produce different polymer environments from weak to strong adsorption scenarios. The free energy of the system and the critical adsorption energy parameter ε_c were investigated via virtual slit-separation moves. It was found that ε_c is a weak function of the chain length for excluded-volume chains (it increases with chain length) for all topologies studied. In a slit with separation comparable or larger than the size of the polymer ($D \geqslant 2R_g$), branched molecules (stars and dendrimers) experience a relatively small entropic penalty for adsorption at low adsorption force due to their compact shape and numerous chain ends, and thus adsorbs better than linear chains of equal molecular weight. However, as the adsorption force increases, the more flexible linear chains reach the compensation point at a weaker attractive energy because of the ease with which monomers can pack closely to the walls. Because of its unique topology and smaller conformational entropy, molecules with intramolecular cross-links, such as cyclic, two-node, and six-node molecules always adsorb more strongly than the other molecules at all adsorption conditions examined. However, in a very narrow slit ($D \leqslant 2R_g$), steric interactions dominate and a similar behavior is observed as that in purely repulsive slits, where molecules with higher intracoil site density (i.e., more compact in size) experience a larger confinement force.

The rest of this paper is organized as follows. In Sec. II, we describe the details of our Monte Carlo simulations. In particular, we explain the confinement force calculation and outline two approaches to locate the critical adsorption point. In Sec. III, we present the simulation results for confinement force, critical adsorption strength, and conformational properties for various polymer topologies at different confinement and adsorption conditions. We conclude in Sec. IV with a few remarks.

II. METHODOLOGY

Polymers are modeled as strings of hard beads of uniform diameter σ. This ''athermal'' molecular model is intended to describe a polymer molecule in a good ''implicit'' solvent; i.e., the preference of polymer sites to be surrounded by solvent rather than by other polymer sites gives rise to an effective repulsive interaction among polymer sites. Some simulations are performed on Gaussian chains, where overlap between polymer sites is allowed, a model appropriate to describe a polymer in a θ solvent. The bond length is allowed to fluctuate within the range 0.85σ–1.15σ and no overlap is allowed between nonbonded spheres; this model can be seen as the continuum-space counterpart of the on-lattice bond fluctuation model commonly used in simulation work [15]. No long-range interactions or bond angle constraints are incorporated; in such a flexible coarse-grained model, each hard sphere represents several actual ''mers'' in a polymer. The simulation box is bounded by two walls perpendicular to the z direction, which extend to infinity in the x and y directions. The polymer-wall interaction is described by the Steele potential [14]

$$U_{\mathrm{bw}}(r) = 2\pi\rho_s\varepsilon(\sigma_{\mathrm{bw}})^2\Delta\left[\frac{2}{5}\left(\frac{\sigma_{\mathrm{bw}}}{r}\right)^{10} - \left(\frac{\sigma_{\mathrm{bw}}}{r}\right)^4 - \frac{\sigma_{\mathrm{bw}}^4}{3\Delta(0.61\Delta + r)^3}\right], \tag{1}$$

where ρ_s is the density of the wall, ε and σ_{bw} are the energy and size parameters, Δ is the separation between planes of molecules inside the wall, and r is the distance between a bead and one of the walls. An overlap distance of $r = 0.2\sigma$ is employed. Since the simulation is done inside a slit, the polymer-wall potential is not truncated. For convenience, we set the values of ρ_s and Δ to 1 (in units of σ^{-3} and σ, respectively), and $\sigma_{\mathrm{bw}} = 0.5$ (in units of σ, based on the assumption that a polymer bead is much larger than a wall site, because in our coarse-grained chain model, a bead represents several polymer monomers). For a given slit separation D, the two slit walls are located at $z = 0$ and D, respectively. The wall potential for a bead at position z can then be calculated as

$$U_w(z) = U_{\mathrm{bw}}(z) + U_{\mathrm{bw}}(D - z). \tag{2}$$

Most of the simulations were performed in the canonical ensemble (constant NVT ensemble) where the slit separation is fixed during the simulation. The molecules are relaxed by hop moves, flip moves, pivot rotations, and translations in the z direction (for details, see our previous paper [9]). In order to improve sampling of chain configurations, parallel tempering is employed [16], where configuration exchanges are carried out among a series of boxes (replicas) with different adsorption strength. This is critical to equilibrate a system with a strong adsorption force, where the chain sites are more likely to be trapped near the walls. In our simulations, seven replicas were typically used over the range from $\varepsilon=0.4$ to 1.8, with more replicas allocated in the critical and strong adsorption regions than in the weak adsorption region. Two parallel tempering moves are carried out between two randomly chosen replica pairs in every Monte Carlo (MC) cycle. During one MC cycle, every site in the polymer moves once on average for every replica box. The force exerted by the polymer chain on the walls is estimated from the change in the Helmholtz potential A when the wall separation is decreased from D to $D-dD$:

$$F=-\left.\frac{\partial A}{\partial D}\right|_{D}. \tag{3}$$

This derivative is evaluated using the virtual-parameter-variation (VPV) method [17]:

$$F=-\left.\frac{\partial A}{\partial D}\right|_{D}=-\frac{1}{\beta}\lim_{\Delta D\to 0}\frac{\ln\langle\exp(-\beta\Delta U)\rangle}{\Delta D}. \tag{4}$$

ΔU is the change of the system energy due to the separation change ΔD, and $\beta=1/k_BT$ where k_b is Boltzmann's constant and T is the temperature. The details of the confinement force calculation can be found in a previous paper [9]. In this study, ΔD ranges from 0 to 0.1. After each virtual slit move, the center of mass of the molecule is rescaled (i.e., it remains at the same reduced z coordinate). Then the whole chain is translated according to its new center of mass, and the energy after the virtual slit move is calculated. The simulation system is relaxed for 1×10^6 cycles and the data are collect over 5×10^6 cycles. For some difficult systems (e.g., linear chains with $N=181$ and 186), a production period of 1×10^7 cycles is used.

The interplay between entropy loss and adsorption enthalpy determines the properties of the confined polymer. On the one hand, conformational entropy loss due to confinement increases the free energy of the system; on the other hand, adsorption enthalpy decreases the free energy. Under critical adsorption conditions ($\varepsilon=\varepsilon_c$), the free energy decrease due to adsorption enthalpy counterbalances the free energy increase due to entropy loss, i.e., the free energy of the confined molecule is identical to that of the free (unconfined) molecule, and thus the partition coefficient between the bulk and the slit is unity ($K=1$). The partition coefficient K is defined as the ratio of polymer concentration in the pore, c_p, to that in the bulk, c_b. In this study, the free energy A of the system and the value of the critical adsorption are determined through the calculation of F as follows. Considering the free energy change of moving isothermally an isolated polymer chain from a free, unconfined bulk environment to a slit with separation D, it follows from Eq. (3) that

$$\Delta A=-\int_{\infty}^{D}F(D')dD'. \tag{5}$$

If, at a certain adsorption strength ε, F equals zero independent of the slit separation (for $D'>D$), then $\Delta A=0$ and $K=1$. This condition thus corresponds to the critical adsorption and $\varepsilon=\varepsilon_c$.

As an alternative approach to evaluating the free energy, an isostress ensemble [18] (constant p_zAT) was also employed. In an isostress ensemble, the pressure normal to the wall (p_z) is fixed while the slit separation is allowed to fluctuate. The probability of a microstate "j" in this ensemble can be expressed as

$$P_j\propto\exp[-\beta(U_j+p_zAD_j)]. \tag{6}$$

The slit separation D is sampled via wall moves, where the position of one wall changes while the positions of the other wall and the polymer inside remain fixed. The location of the critical adsorption parameter ε_c can be identified by the point where the average slit separation $\langle D\rangle$ equals $1/\beta P_zA$; this criterion is based on the fact that in the absence of either confinement or adsorption effects (i.e., a polymer in an infinitely large slit), the polymer should approach ideal behavior, wherein $\beta P_zA\langle D\rangle=1$.

Six different model molecules were employed in this study, namely, linear, cyclic, star, dendritic, two-node, and six-node molecules. Schematic representations of the topology of these molecules are given in Fig. 1. The stars and dendrimers are chosen to investigate the branching effect on confinement/adsorption behavior. The star polymers employed have four arms, i.e., $f=4$. The dendrimers under study have a central core that branches off into three arms. Each arm branches into two additional branches; the number of bonds between branched points (i.e., the separator length) is 4. The generation number ranges from 1 to 3. The size of these model molecules ranges from $N=37$ to 181. Two- and six-node molecules ($N=186$) are employed to study the effect of intramolecular cross-linking. The two-node molecule employed has two tetrafunctional cross-linking nodes and four strands, each having 46 sites ($N_{\mathrm{str}}=46$), and the six-node molecule has six nodes and 12 strands with $N_{\mathrm{str}}=15$. The cyclic molecule also fits loosely into this category with one bifunctional cross-linking. Note that the ratio of the number of bonds to the number of sites ($\equiv r_b$) for a molecule with N beads is $(N-1)/N<1$ for the linear, star, and dendrimer chains, while it is 1, $(N+2)/N$, and $(N+6)/N$ (i.e., $r_b\geqslant1$) for the cyclic, two-node, and six-node molecules, respectively. The coil sizes in the bulk (R_g^0) of all the molecules employed were obtained via simulation and are shown in Table I.

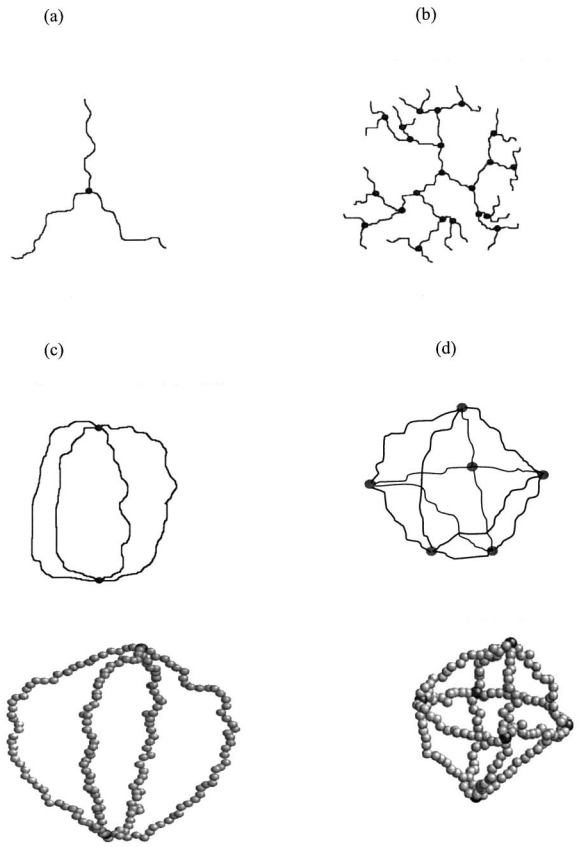

FIG. 1. Schematic representation of some of the topologies employed in this study. (a) star, (b) dendrimer, (c) two-node molecule, and (d) six-node molecule. The beads in (a) and (b) represent branching nodes having more than two bonds; black beads in (c) and (d) represent tretrafunctional cross-links.

III. SIMULATION RESULTS

The effect of slit separation on adsorption behavior was investigated first. In Fig. 2(a), the confinement force βF is plotted as a function of slit separation at different adsorption strengths ε for a linear chain with $N=85$. As the attraction intensifies between the walls and the polymer, the confinement force decreases, from positive values at weak adsorption to negative values at strong adsorption. At weak adsorption, βF decreases with increasing D and approaches zero from above; at strong adsorption, βF increases with D and approaches zero from below. At $\varepsilon=\varepsilon_c=1.4$, the βF vs D curve is flat with $\beta F\sim 0$ for all D values (within the simulation uncertainty); similar results were also seen for other chain lengths and chain types. As discussed in the preceding section, this finding justifies our approach of using $\beta F=0$ as the criterion for critical adsorption. To further test this idea, the value of chemical potential of the same chain at ε_c is obtained from Widom's chain insertion method [19,20], where a chain is inserted segment by segment in a configurational-biased fashion, and plotted as a function of D in Fig. 2(b). It is observed that, except for the very narrow slit ($D<2R_g^0$), the chemical potential of the chain in the slit remains constant and essentially equals the bulk value (shown by the dashed line) within simulation error. In other words, ε_c is independent of slit separation for a molecule in a relatively large slit ($D>2R_g^0$) (i.e., moderate to weak confinement), which is the case in most practical applications (e.g., the tube size is usually larger than that of the molecules in liquid chromatography).

TABLE I. Coil sizes in the bulk (R_g^0, in units of σ) for molecules employed in this study.

	$N=85$	$N=181$	$N=186$
Linear chain	6.82	10.92	11.1
Cyclic chain	5.07	8.06	8.19
Star	5.28	8.45	
Dendrimer	4.36	5.74	
Two-node molecule			6.04
Six-node molecule			4.98

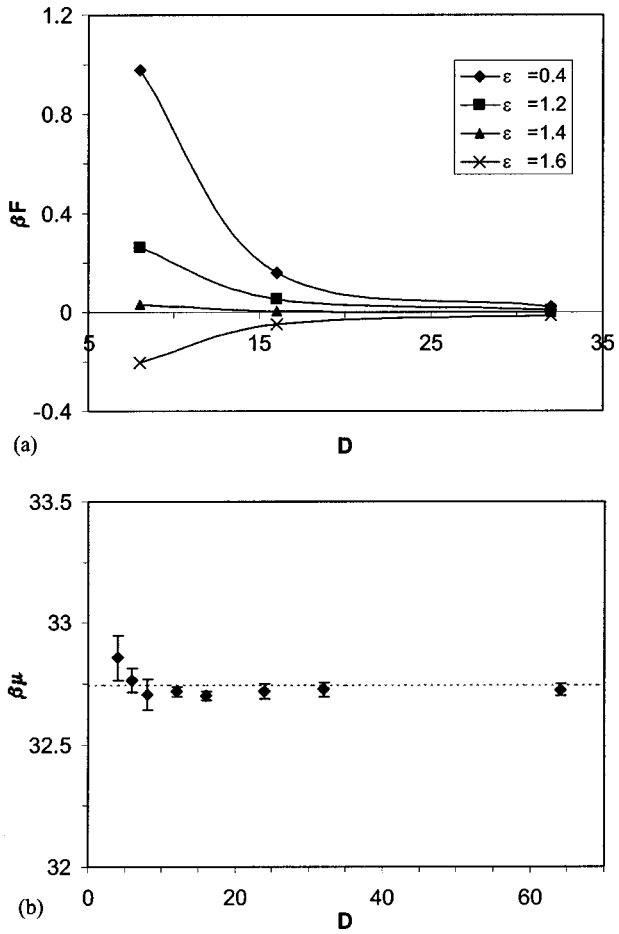

FIG. 2. (a) Confinement force βF as a function of slit separation D for different adsorption strengths ε for linear chain with $N=85$. (b) Chemical potential values for the same chain obtained from Widom chain-insertion method at ε_c. The dashed line indicates $\beta\mu$ in the bulk.

Based on theoretical grounds [10], the critical adsorption strength for a linear Gaussian polymer is predicted to be independent of chain length. For linear chains with EV interactions, however, ε_c was found to be chain-length dependent

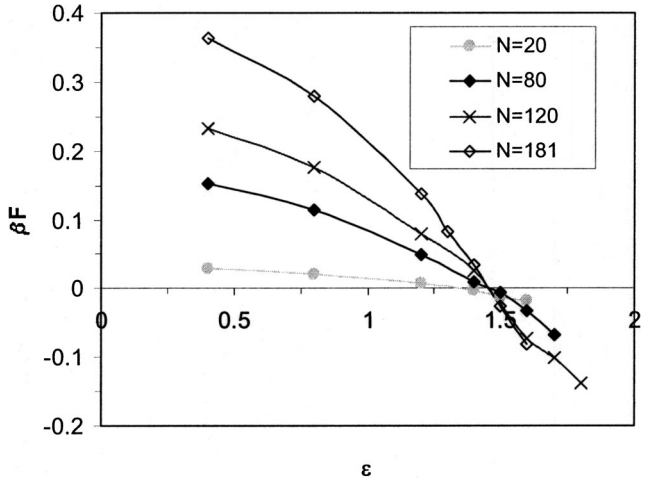

FIG. 3. Confinement force βF as a function of adsorption strength ε for linear chains with lengths from $N=20$ to 181 at $D=16$. Simulation error bars are commensurate to the symbol sizes and lines are drawn to guide the eye.

in an on-lattice simulation [11]. In Fig. 3, the confinement force βF at different adsorption strengths ε is plotted for linear chains with lengths from $N=20$ to 181 in the same slit with $D=16$. As the chain length increases, a small but noticeable increase in the value of ε_c is observed; it varies from $\varepsilon_c=1.37$ for $N=20$ to $\varepsilon_c=1.46$ for $N=181$, which agrees qualitatively with previous findings [18]. The dependence of ε_c on chain length was also observed for other chain architectures (results not shown).

Chain topology is expected to have an important effect on the interplay between entropy loss and adsorption enthalpy. In Fig. 4, the adsorption behavior of linear, cyclic, star, and dendrimer molecules of the same molecular weight ($N=85$) and in the same slit ($D=16$) is examined by comparing their βF vs ε curves. Considering that the coil sizes ($2R_g^0$) of all the molecules are smaller than D, this scenario corresponds to moderate confinement. Results for Gaussian chains are shown in Fig. 4(a). From weak to critical adsorption strength, dendrimers adsorb better (i.e., experience a smaller confinement force) than star and linear chains, with linear chains being at the opposite end. This behavior can be explained by the bulk coil size (R_g^0) difference among these chains, where dendrimers have the most compact size and linear chains have the most extended configuration (see Table I). Molecules with small coil size suffer less entropy loss upon moderate confinement in the slit and thus adsorb better (see [9]). As the adsorption force is intensified, however, the differences in confinement force among these three molecules diminish. In strong adsorption conditions, their curves almost overlap. Because Gaussian chains can adopt collapsed configurations as they attach to a strongly attractive wall, the difference in molecular topology plays a negligible role in adsorbing behavior. As a clear departure from the above behavior, the cyclic molecule, with a bulk coil size larger than that of the dendrimer, always adsorbs much better than the other molecules, even at strong adsorption conditions. This unique phenomenon is due to the molecular topology of the cyclic molecule. When attracted near the wall,

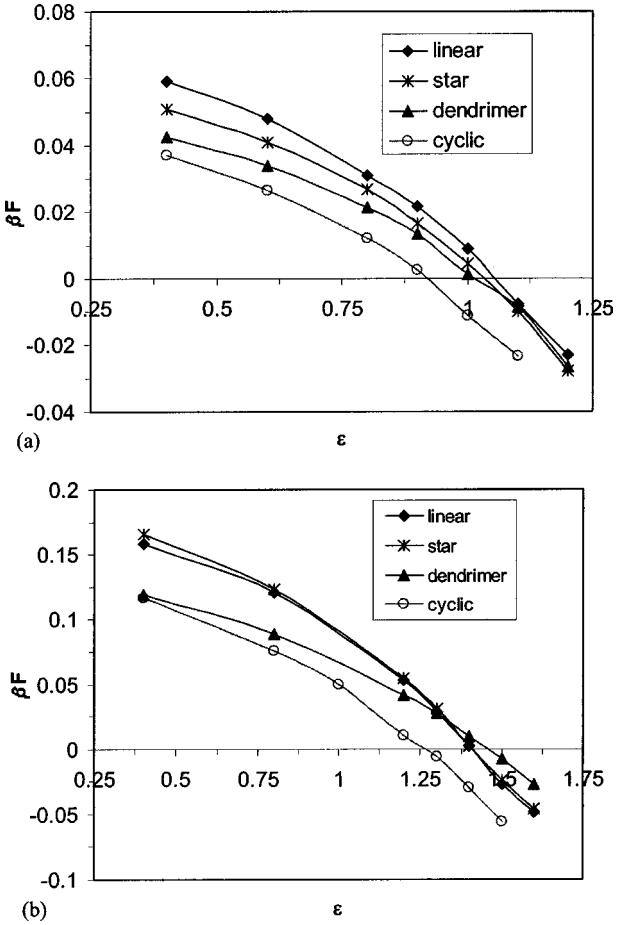

FIG. 4. Confinement force βF as a function of adsorption strength ε for linear chain, star, and dendrimer with $N=85$ in a slit with $D=16$. (a) Gaussian and (b) EV chains.

the ring molecule suffers the least conformational entropy loss. These cyclic chain results illustrate that, while larger R_g^0 is usually associated with larger molecular conformational entropy (and thus larger entropy loss upon confinement), R_g^0 alone is not a complete indicator of such entropy.

The βF vs ε curves for EV chains are shown in Fig. 4(b). The curve for stars almost overlaps with that for the linear chains. At weak adsorption, dendrimers adsorb better than stars and linear molecules, again due to the coil size difference. But when approaching the critical adsorption condition, the adsorption of a dendrimer become less favorable and it requires a larger adsorption strength to reach the critical point. Because of excluded-volume interactions, a dendrimer, unlike the more flexible linear and star chains, cannot easily adopt flat configurations to maximize the contacts with the wall even for strong adsorbing interaction. Cyclic molecules still adsorb better that the other three molecules because of its unique topology. The site density profile of these molecules across the slit is shown in Fig. 5 for strong adsorption force ($\varepsilon=1.4$, close to ε_c). Two distinguishable peaks located 1 σ apart can be observed near the walls, which indicates a layered structure induced by the strong adsorption. In the region close to the wall, the linear chain

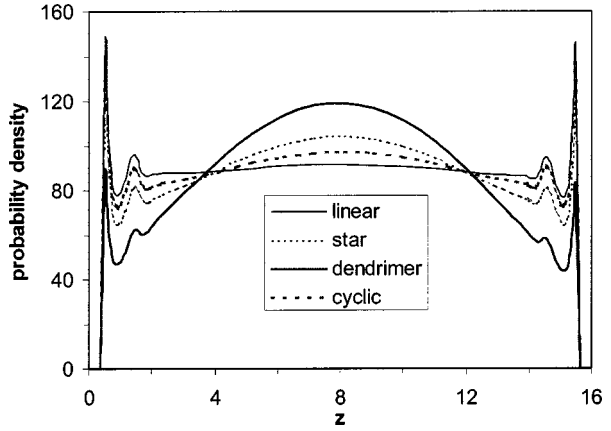

FIG. 5. Bead density profiles for linear, star, dendrimer, and cyclic molecules with $N=85$ across a slit with $D=16$ at $\varepsilon=1.4$.

has the largest site density, followed by the cyclic chain, star, and dendrimer.

βF vs ε curves for longer chains with $N=181$ and in a slit with $D=16$ are shown in Fig. 6(a). In this case, the slit separation is comparable to the coil size of the molecules, which corresponds to the strong confinement scenario. Consequently, dendrimer and star molecules will experience more entropy loss because of their higher inner monomer density (see [9]), which leads to larger confinement forces than for linear chains in weak adsorption conditions. This trend is contrary to that observed for molecules with $N=85$ at $D=16$. When the steric confinement is still the dominant factor (i.e., weak adsorption), the slit separation, or more specifically the ratio of R_g^0 to D, has a significant effect on the confinement behavior of molecules with different topology. As the adsorption force increase, the three curves seems to converge and reach the critical point at the same ε_c. Figure 6(b) shows the results of these chains in a large slit ($D=32$). Similar behavior was observed as that for chains with $N=85$ in a slit with $D=16$ [Fig. 4(b)]. With a weak adsorption force, a linear chain exerts the largest F on the walls, followed by the star, cyclic molecule, and dendrimer, which is consistent with their R_g^0 values. As the adsorption force increases, the F curve of the dendrimer crosses that of the cyclic chain first, and then those of the linear chain and the star. As a result, the value for ε_c is largest for the dendrimer and smallest for the cyclic chain.

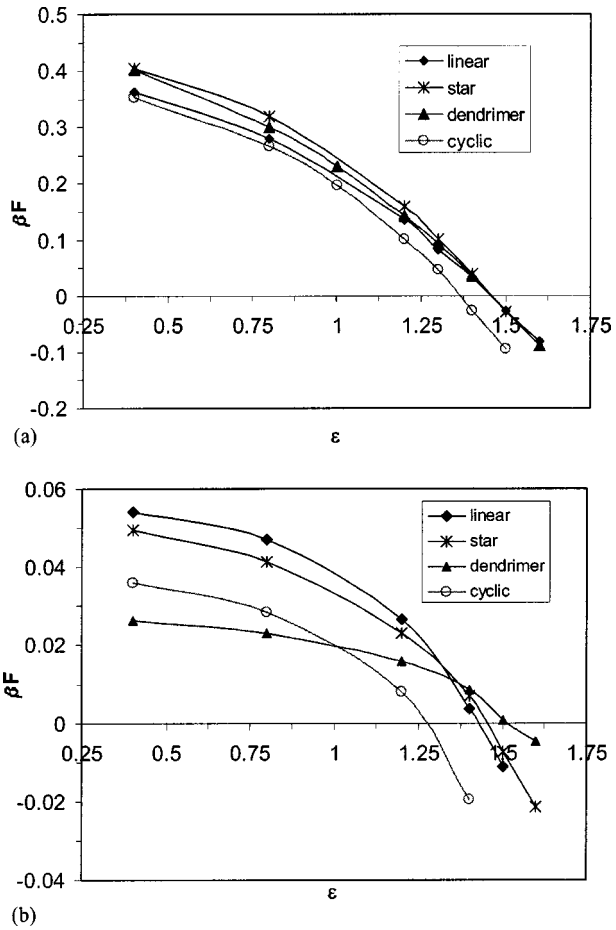

FIG. 6. Confinement force βF as a function of adsorption strength ε for linear chain, star, dendrimer, and cyclic molecules with $N=181$ in a slit with $D=$(a) 16 and (b) 32.

As observed in the above, cyclic molecules exhibited a unique adsorption behavior compared to linear chains and branched molecules (stars and dendrimers). For example, cyclic molecules always have the smallest ε_c value. One possible explanation is that a cyclic molecule can be seen as a linear chain connected from head to tail (i.e., one intramolecular cross-link). Such an intramolecular cross-linking reduces the number of available configurations for cyclic molecule in solution (conformational entropy). It can be argued that when a molecule with such intrinsic topological constraints is confined in a not-too-narrow slit, it will suffer less entropy loss and thus require a smaller adsorption strength to achieve critical adsorption (compared to topologically unconstrained chains). To test this hypothesis, we investigated the confinement/adsorption behavior of ''model'' molecules with more intramolecular cross-linking: namely, a two-node molecule and a six-node molecule wherein a node refers to a tetravalent site (see Fig. 1). Each molecule has 186 total sites. In Fig. 7(a) the results for moderate confinement ($D=32$) are shown and compared to those of linear and cyclic chains with the same molecular weight. In accord with the hypothesis, the six-node molecule has the smallest confinement force under all adsorption conditions and reaches critical adsorption at the weakest adsorption strength, followed by the two-node, cyclic, and linear molecules. Keeping in mind that at moderate to weak confinement ε_c is independent of slit separation, the R_g^0/D ratio is irrelevant in the discussion of the critical adsorption condition. Figure 7(b) shows the results in a narrow slit ($D=8$) where steric confinement is expected to dominate the confinement/adsorption behavior. Because the six-node molecule has the highest intracoil site density, it has the largest confinement force under all adsorption conditions, followed by the two-node, cyclic, and linear molecules. Notice that the curves for linear and cyclic molecules overlap very well, which suggests that the topology difference between them is no longer important in the presence of a very strong confinement ($D \ll 2R_g^0$ for both chains).

The site density profiles for linear, cyclic, two-node, and

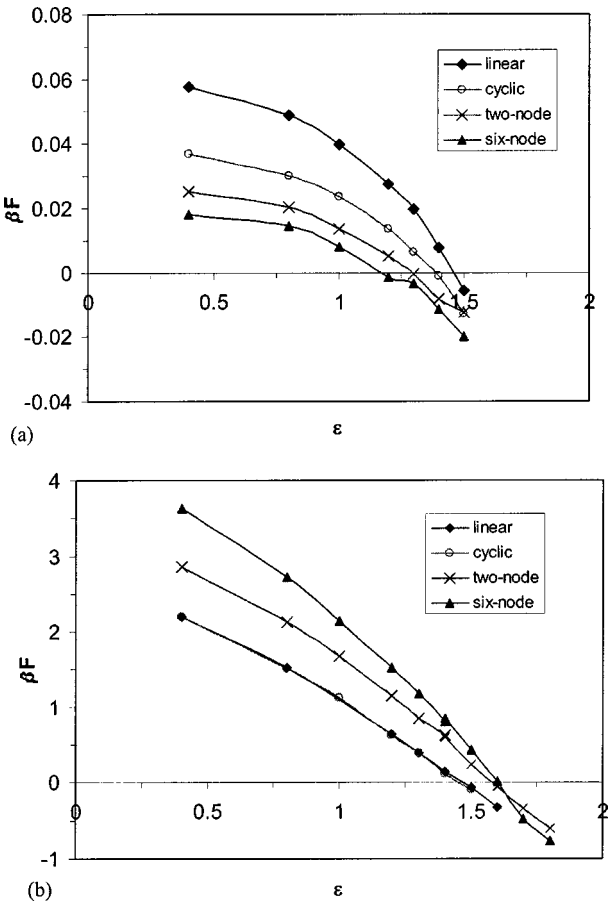

FIG. 7. Confinement force βF as a function of adsorption strength ε for linear, cyclic, two-node, and six-node molecules with $N=186$ in a slit with $D=$(a) 32 and (b) 8.

six-node molecules across a slit with $D=32$ at $\varepsilon=1.4$ (strong adsorption) are shown in Fig. 8. In the double-layer structure adjacent to the walls, the six-node molecule has the largest peak height (i.e., largest site concentration), followed by the two-node, cyclic, and linear molecules. Such a trend is in completely reverse order to that corresponding to weak adsorption, where the linear chain has the highest density close

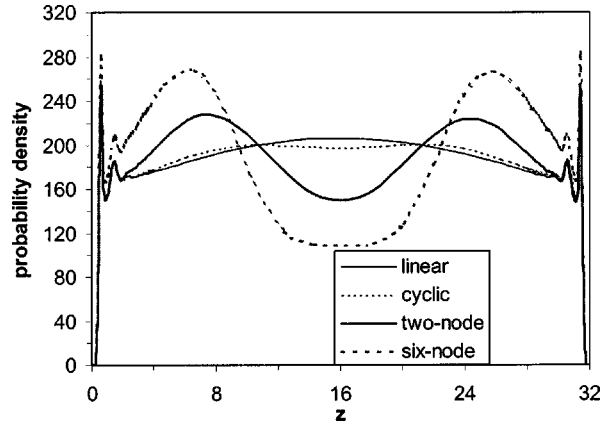

FIG. 8. Site density profiles for linear, cyclic, two-node, and six-node molecules with $N=186$ across a slit with $D=32$ at $\varepsilon=1.4$.

to the wall and the six-node molecule has the lowest (not shown). In the region near the walls, six- and two-node molecules form a large third peak, where the site density is much higher than that in the middle of the slit. Induced by the adsorption force, these two multinodal molecules tend to be highly localized near the walls. The location of that third peak correlates with the center of mass position of the molecule. Apparently, more sites near the wall results in a large adsorption enthalpy, which reduces the confinement force.

Confinement forces can also be related to depletion forces in dilute polymer colloid mixtures [21] if the colloidal particles are so much larger than the polymer coils that their surfaces can be approximated by planar walls [22]. Because F relates to the osmotic pressure difference between the bulk solution and the confined zones, a positive F indicates that polymers will tend to be excluded from the gap (of separation D) between two colloidal particles and "push" the particles together (depletion attraction). On the contrary, a negative F indicates a polymer-mediated repulsion between colloidal particles that provides steric stabilization. In addition to the polymer-wall interaction strength ε, our simulations show that polymer topology could also be used to control F and thus the colloidal phase behavior. For equal N, linear chains should be more efficient depleting agents (larger positive F values for non- or weak-adsorption conditions), while intra-cross-linked molecules should be more effective stabilizers (smaller, more negative F values at a given ε and a lower threshold "ε_c" for steric stabilization).

To analyze the conformational behavior of a polymer confined in an attractive slit, it is important to consider two phenomena, a collapse effect (unilateral clustering) and a bridge effect (bilateral clustering).

(1) The collapse effect occurs when the molecule is attracted toward one of the (strongly attractive) walls and collapses into a nearly two-dimensional configuration. This effect will result in an increase in $R_g(x,y)$ and a decrease in $R_g(z)$.

(2) The bridge effect occurs when the coil size of the molecule is comparable to the slit separation; it is then possible that the same molecule attaches to both walls and forms a bridge between them. This effect will induce an increase in $R_g(z)$ and a decrease in $R_g(x,y)$.

A cartoon representation of these two effects is shown in Fig. 9. In Fig. 10, R_g, $R_g(x,y)$, and $R_g(z)$ for a linear chain with $N=181$ are plotted as functions of ε. As expected, R_g and its components are nonmonotonic functions of ε and exhibit different behavior at different slit separations, which can be explained by the competition between the collapse and bridge effects. In narrow slits with separation less than $2R_g^0$ (i.e., $D=8,16$), the bridge effect dominates and $R_g(z)$ increases over the whole ε range studied. In large slits (e.g., $D=32$), $R_g(z)$ first increases slightly with ε due to the bridge effect, and then decreases, beginning from the critical adsorption point on. At all slit separations, $R_g(x,y)$ decreases first and then increases abruptly. Notice that the turning point is coincident with the critical adsorption point, suggesting that it is possible to estimate the critical adsorption point by tracking the conformational behavior.

To show that our results for fixed-D slits are consistent

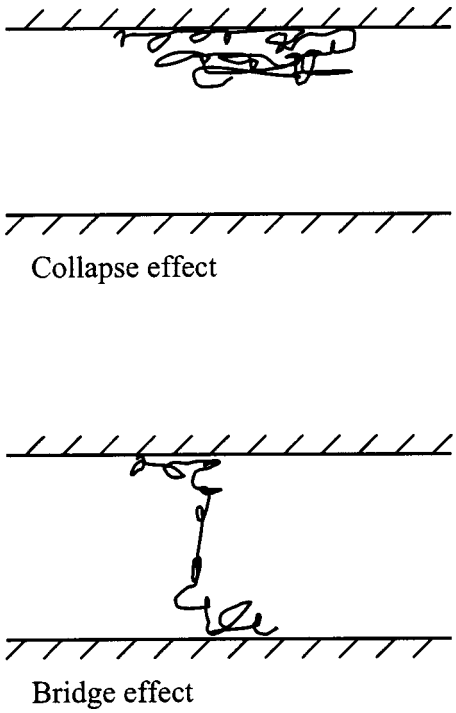

FIG. 9. Cartoon drawings of chain configurations in an adsorptive slit due to collapse effect and bridge effect, respectively.

with those where fluctuations in D are allowed, isostress ensemble simulation data are shown in Fig. 11 for linear, star, dendrimer, and cyclic molecules with $N=85$. The confinement force applied is $\beta P_z A=0.0625$. Figure 11(a) shows the average slit separation $\langle D\rangle$ as a function of adsorption force ε. As the adsorption force increases, $\langle D\rangle$ decreases. With a weak adsorption force, $\langle D\rangle$ for the linear chain is the largest, followed by those for the star and dendrimer chains. However, with a strong adsorption force this trend is reversed: the dendrimer has the largest $\langle D\rangle$, followed by the star and linear chains. The cyclic molecule always has the smallest $\langle D\rangle$. When $\langle D\rangle=1/(\beta P_z A)$ (indicated by the dashed line), molecules reach the critical adsorption point (ε_c). In increasing order, the value of ε_c goes as cyclic chain<linear chain <star<dendrimer, which is consistent with results from the confinement force calculations shown earlier. However, there are some discrepancies between the precise values of ε_c from these two methods: ε_c from isostress simulations is slightly larger than that from confinement force calculations. Such differences reflect the different physical scenarios described by these methods. Distributions of D in isostress simulations are surprisingly broad, as shown in Fig. 11(b) for a star molecule. Such large fluctuations in D around $\langle D\rangle$ would likely diminish if simulations were performed for multiple confined chains (noninteracting among themselves to mimic highly dilute conditions). It is further observed in Fig. 11(b) that, as the adsorption force increases, the D distribution becomes narrower and shifts to the left (smaller $\langle D\rangle$).

IV. CONCLUSIONS

In this paper, the confinement/adsorption behavior of topologically complex polymers in adsorptive slits has been investigated. Geometrical confinement was introduced by placing an isolated polymer chain inside a slit-pore. The polymer-wall interaction is described by the Steele potential. The simulations were performed in the NVT ensemble and the confinement force, monomer density profile, and conformational properties were collected and analyzed as a function of adsorption strength. It was found that, in moderate to weak confinement, the confinement force vanishes at the same adsorption strength (ε_c) for a given molecule, independent of slit separation. This finding justifies our approach of

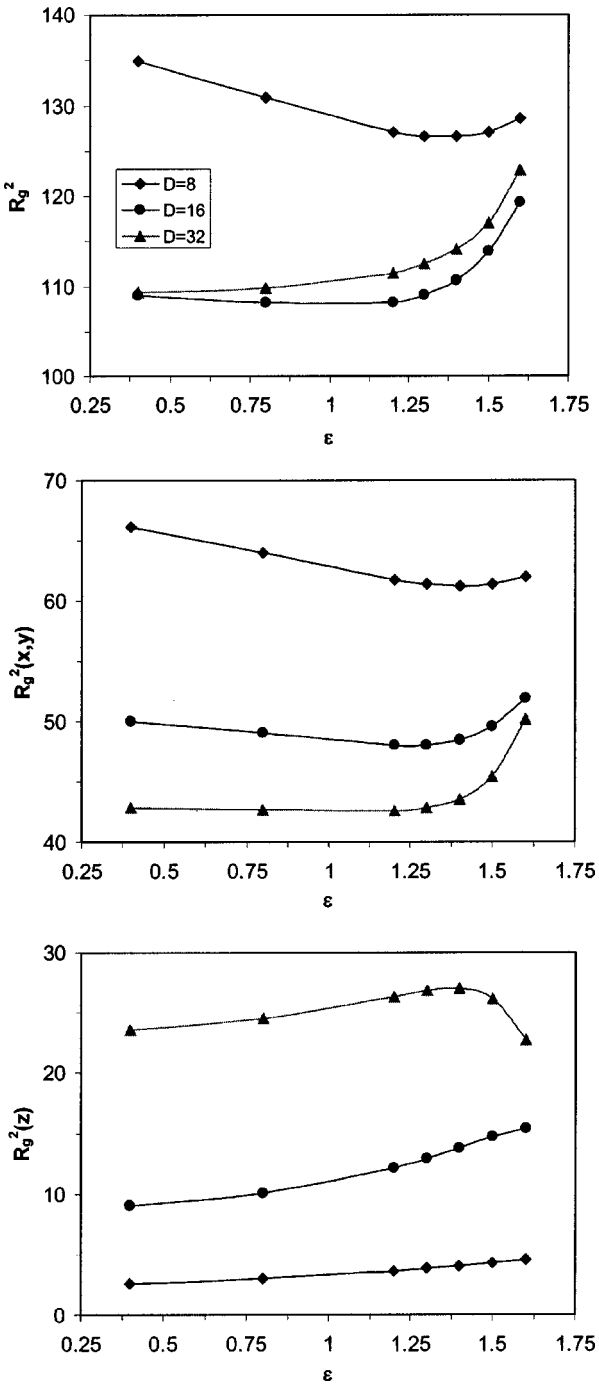

FIG. 10. Conformational properties for a linear chain with $N=181$ in slits (with $D=8$, 16, and 32, respectively) as a function of adsorption strength ε.

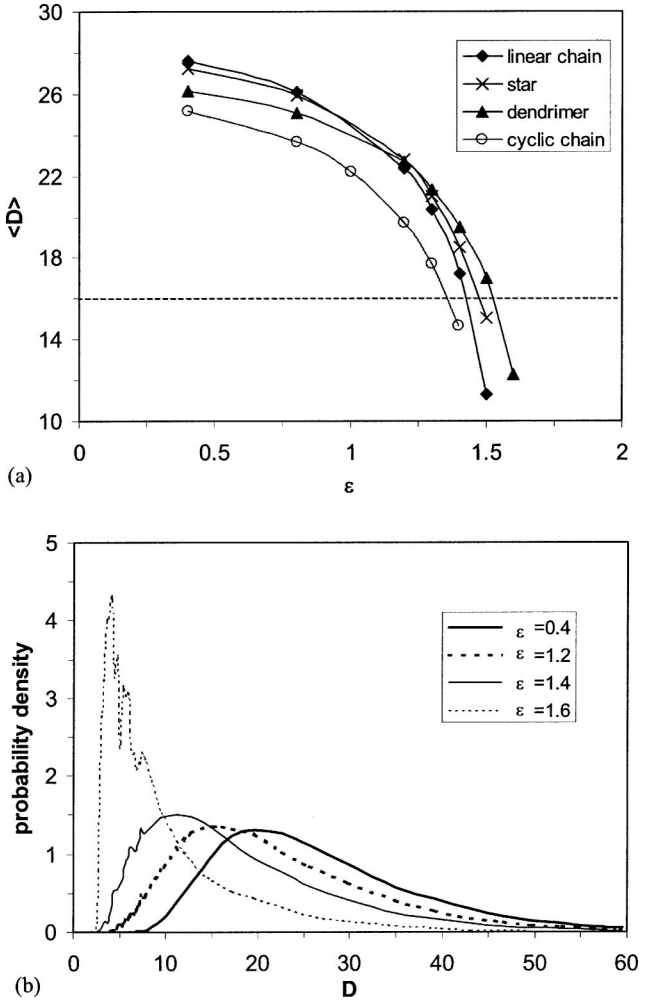

FIG. 11. (a) Average slit separation $\langle D \rangle$ as a function of adsorption force ε for linear chain, star, dendrimer, and cyclic molecules with $N=85$. The confinement force applied is $\beta P_z A=0.0625$. When $\langle D \rangle = 1/(\beta P_z A)$ (indicated by dashed line), molecules reach the critical adsorption point (ε_c). (b) Distance distributions for stars in isostress simulations.

using $\beta F=0$ as the criterion for critical adsorption. For excluded-volume chains, it was found that ε_c is a weak function of chain length.

Two classes of chain topology were studied: (i) branched polymers, including stars and dendrimers; and (ii) chains with intramolecular cross-links, such as cyclic, two-node, and six-node molecules. Under very strong confinement ($D < 2R_g^0$), steric effects (packing entropy) dominate the interplay between confinement and adsorption, so that chain rigidity (i.e., intracoil site density) is the main contributor to the confinement force and chain free energy. This trend is analogous to that observed in a purely repulsive slit. However, chain topology has a major impact on the interplay of entropy loss and adsorption enthalpy in moderate to weak confinement. For equal molecular weights, branched molecules, such as the star and dendrimer, adsorb better in weak adsorption conditions because of their compact coil size. However, as the adsorption intensifies, the more flexible linear chain spreads closer to the walls and reaches the critical condition at a weaker adsorption force. Because of their topological constraints, molecules with intramolecular cross-links, such as cyclic, two-node, and six-node molecules, have smaller conformational entropy, and thus experience less entropy loss upon confinement. Consequently, in moderate to weak confinement, these molecules always adsorb more strongly than the linear and branched molecules under all adsorption conditions examined, and the more constrained is the topology, the better is the adsorption. The two- and six-node molecules tend to be localized near a wall for strong adsorption forces.

Results from this paper could be useful for processes involving polymers in the critical and adsorption regimes that exploit differences in molecular architecture (in addition to molecular weight); e.g., for polymer separations and colloidal stabilization. The complex behavior due to the interplay between chain topology, steric confinement, and wall adsorption can be used to guide the optimal choice of confinement and adsorption conditions. Branching and intramolecular cross-linking affect the confinement/adsorption behavior differently, and it might be possible to tune separation resolution or depletion interactions by introducing agents that temporarily and reversibly induce a change of molecular topology. For example, the elution time of a molecule can be increased by inducing intramolecular cross-links. The availability of pores with well-defined geometry and the ability to manipulate single molecules will facilitate future experimental studies of polymer adsorption which could test and complement our simulation results.

ACKNOWLEDGMENT

This work was supported by the U.S. Department of Energy, Grant No. DE-FG02-02ER15291.

[1] E. F. Cassaca, J. Polym. Sci., Part B: Polym. Lett. **5**, 773 (1967).
[2] L. Turban, J. Phys. (France) **45**, 347 (1984).
[3] P.-G. de Gennes, *Scaling Concepts in Polymer Physics* (Cornell University Press, Ithaca, NY, 1979).
[4] A. A. Gorbunov and A. M. Skvortsov, Vysokomol. Soedin., Ser. A **29**, 926 (1987).
[5] A. M. Skvortsov and A. A. Gorbunov, Vysokomol. Soedin., Ser. A **28**, 1686 (1986).
[6] A. M. Skvortsov and A. A. Gorbunov, J. Chromatogr. **507**, 487 (1990).
[7] A. Sikorski, Macromol. Theory Simul. **10**, 38 (2001).
[8] R. Yerushalami-Rozen, B. J. Hostetter, L. J. Fetters, and J. Klein, Macromolecules **23**, 2984 (1990).
[9] Z. Chen and F. A. Escobedo, Macromolecules **34**, 8802 (2001).
[10] A. A. Gorbunov and A. M. Skvortsov, Adv. Colloid Interface Sci. **62**, 31 (1995).
[11] P. Cifra and T. Bleha, Polymer **41**, 1003 (2000).

[12] Y. Gong and Y. Wang, Macromolecules **35**, 7492 (2002).
[13] C. M. Guttman, E. A. Di Marzio, and J. F. Douglas, Macromolecules **29**, 5723 (1996).
[14] W. A. Steele, *The Interaction of Gases with Solid Surfaces* (Pergamon, Oxford, 1974).
[15] I. Carmesin and K. Kremer, Macromolecules **21**, 2819 (1988).
[16] K. Hukushima and K. Nemoto, J. Phys. Soc. Jpn. **65**, 1604 (1996).
[17] H. L. Vörtler and W. R. Smith, J. Chem. Phys. **112**, 5168 (2000).
[18] F. A. Escobedo, J. Chem. Phys. **115**, 5642 (2001).
[19] M. N. Rosenbluth and A. W. Rosenbluth, J. Chem. Phys. **96**, 2395 (1955).
[20] D. Frenkel, G. C. A. M. Mooji, and B. Smit, J. Phys.: Condens. Matter **3**, 3053 (1992).
[21] T. Bleha and P. Cifra, Polymer **44**, 3745 (2003).
[22] S. Asakura and F. Oosawa, J. Chem. Phys. **22**, 1255 (1954).